

## Full length article

# Yb:KGW self-Raman laser with $89\text{ cm}^{-1}$ Stokes shift and more than 32% diode-to-Stokes optical efficiency

Merilyn S. Ferreira, Niklaus U. Wetter\*

Centro de Lasers e Aplicações, IPEN-CNEN/SP, Av. Professor Lineu Prestes, 2242 São Paulo, SP, Brazil



## HIGHLIGHTS

- Yb:KGW self-Raman laser system with very high slope efficiency of  $42 \pm 8\%$ .
- Highest output power achieved from a self-Raman laser based on Yb:KGW.
- Prospects of obtaining a frequency comb of modes spaced by  $89\text{ cm}^{-1}$ .

## ABSTRACT

We report on a Yb<sup>3+</sup>:KGW self-Raman laser operating at 1096 nm. A 100 μm fiber-coupled diode end-pumped configuration is used to generate a fundamental emission wavelength that strongly depends on internal resonator losses. Stokes emission at 1096 nm is achieved with a slope efficiency of  $42 \pm 8\%$ , an optical conversion efficiency of more than 32% and a maximum output power of 4.5 W for quasi-continuous operation (1 ms pulses). The explored Stokes conversion of  $89\text{ cm}^{-1}$  shows excellent laser characteristics, indicating that this still little explored Stokes shift could pave the way to continuous-wave Raman frequency-comb lasers.

## 1. Introduction

Self-Raman lasers (SRLs) are the Raman lasers of lowest cost and they allow simple and compact set-ups. In these lasers, the fundamental laser transition and the stimulated Raman scattering (SRS) occur in the same crystal, thus, the amount of optical components in these cavities is smaller than in cavities with separate crystals for fundamental and Stokes wavelengths generation, consequently reducing the intracavity losses and providing, in principle, higher efficiency. There are two characteristics that can hamper self-Raman lasers: first, the difficulty to optimize independently the mode size of the fundamental laser, and also of the Raman laser, at the laser crystal in order to achieve the best coupling between fundamental and Stokes fields. The second limiting problem is the thermal load, since self-Raman crystals will accumulate not only the thermal load induced by the quantum defect, but also the thermal load induced by inelastic scattering responsible for the generation of the Raman wavelength. The combination of both thermal loads tends to limit the power obtained by these lasers.

Self-Raman lasing has been demonstrated for Nd<sup>3+</sup> doped crystals using mainly vanadates, such as GdVO<sub>4</sub> and YVO<sub>4</sub>, and double-metal-tungstates, such as KGd(WO<sub>4</sub>)<sub>2</sub> (KGW) and KY(WO<sub>4</sub>)<sub>2</sub> (KYW) [1–4]. However, Nd<sup>3+</sup> doped materials suffer from parasitic losses such as

upconversion losses, especially at the high pump intensities needed for Raman gain and, therefore, suffer from relatively lower efficiency and higher thermal load when compared to ytterbium doped materials [5]. Yb<sup>3+</sup> ions have a simpler energy level diagram and, in consequence the parasitic losses are reduced, offering significant advantages when compared to Nd<sup>3+</sup> lasers at 1.06 μm. They also have a much smaller quantum defect than Nd<sup>3+</sup> lasers, because they may be pumped at 940 nm or 980 nm, which allows producing lasers with intrinsically high slope efficiency and much smaller thermal load at equivalent pump power. Moreover, the long upper state lifetime of ~1 ms and broad absorption bandwidth observed in many ytterbium doped hosts is prone to diode pumping. Due to these qualities, a vast number of works on Yb-doped diode-pumped solid-state lasers have been demonstrated.

KGW presents Raman shifts with large SRS cross-sections at  $89\text{ cm}^{-1}$ ,  $768\text{ cm}^{-1}$  and  $901\text{ cm}^{-1}$  [6]. Of those, the  $89\text{ cm}^{-1}$  cross-section presents the highest SRS cross-section for Ng-axis cut crystals and the favorable characteristic of less crystal heating due to the smaller Raman shift, which allows higher pump powers [7]. The higher gain coefficient of approximately 9.2 cm/GW may be, in part, attributed to the longer dephasing time of the shorter Stokes shift [7]. Stokes heating in SRLs has been estimated for Nd:GdVO<sub>4</sub> and amounts to approximately 20% for the  $873\text{ cm}^{-1}$  Raman shift in this crystal [8]. The

\* Corresponding author.

E-mail address: [nuwetter@ipen.br](mailto:nuwetter@ipen.br) (N.U. Wetter).

much smaller  $89\text{ cm}^{-1}$  Raman shift has, therefore, negligible influence in the total heat deposited into the crystal. Raman lasers typically have a gain coefficient of around  $5\text{ cm/GW}$ , which requires very high intracavity intensities for the fundamental and Stokes wavelength in order to maintain SRS lasing. Especially for CW operation, it is of fundamental importance to keep the losses small, which includes the necessity of mirror coatings with reflectivity of ideally more than 99.9% at the fundamental and first Stokes wavelength, as well as crystal coatings with less than 0.1% transmission per surface at both wavelengths. This is much easier to achieve for smaller Stokes shifts, and the increase in mirror reflectivity immediately translates in higher SRL efficiency.

There are few works of ytterbium doped hosts that showed SRL action, among which Yb:KGW predominates in terms of published works [9–12]. Yb:KGW has shown to be an excellent candidate for laser operation at the fundamental wavelength because of its large stimulated emission cross section ( $2.8 \times 10^{-20}\text{ cm}^2$  at 1026 nm), small quantum defect ( $\cong 5\%$ ) and acceptable Stark level structure [10]. Like most ytterbium hosts, it has a small energy separation between the lower laser level and the ground-state that causes a significant thermal population of this level at room temperature, giving the laser quasi-three-level characteristics, including reabsorption of laser wavelength at room temperature that causes a significant increase in the laser threshold. Because of this quasi-three-level nature, Yb:KGW has strongly overlapping emission and absorption bands, and laser action can be observed from 1025 nm to 1090 nm depending on cavity losses [10]. As a favorable characteristic, its wide absorption band is well matched to the emission spectrum of high power InGaAs 940 nm and 980 nm diode lasers (see Fig. 1a).

Most of the demonstrated ytterbium-SRLs have been operated in pulsed mode and on the larger Raman shifts. To our knowledge, the first and only ytterbium-SRL operation at the shorter wavelength mode of  $89\text{ cm}^{-1}$  was demonstrated in 2013, resulting in a maximum CW

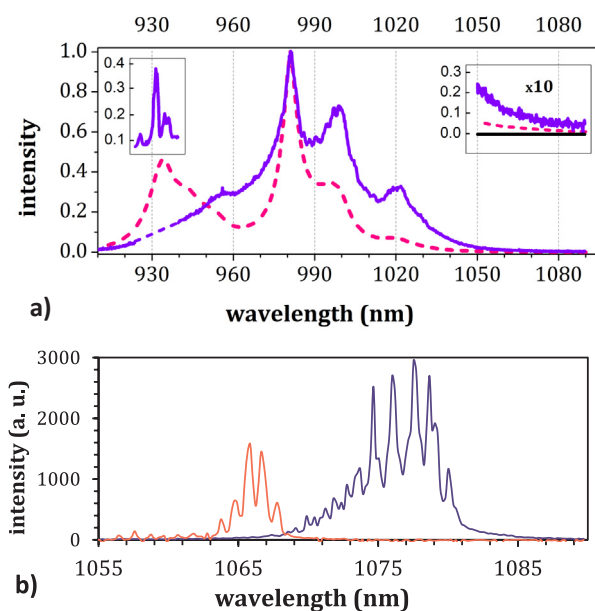


**Fig. 1.** (a) Normalized absorption (dashed line) and emission (solid line) spectra of Yb:KGW. Left inset: diode emission spectrum at maximum pump power, peaked at 934 nm and subtracted from the emission spectra (where the dashes appear in the emission curve). Right inset:  $\times 10$  absorption and emission in the interval between 1050 nm and 1090 nm. The black line corresponds to zero absorption and emission intensity. Both insets use the same x-scale as the bottom x-scale and the y-scale is in normalized units. (b) Two different emission spectra of the fundamental laser (both using the same y-scale of arbitrary units) with their different center wavelength depending on the alignment of the cavity; a better alignment results in a longer center wavelength of the spectrum.

Raman output power of 1.7 W, with slope efficiency and diode-to-Stokes optical conversion efficiencies of 26.6% and 21.8%, respectively [13].

In this work we present, what is to our knowledge, the highest efficiency and peak output power for an Yb-doped self-Raman laser.

## 2. Materials and methods

In order to achieve high efficiency in the presence of reabsorption, we resorted on MATLAB simulations [14,15], which had been made for previous works on three-level lasers and Raman lasers [16–18]. The simulations served only as general guidelines, once the complex multimode behavior of the fundamental level under the effect of depletion caused by the Stokes emission, as well as other influences, could only be estimated [19]. However, we found that a shorter crystal with less doping is preferable when compared to previous results [13]. The high gain SRL demonstrated in this work could be of interest for multi-wavelength laser sources by obtaining several higher order Stokes modes that are closely spaced by  $89\text{ cm}^{-1}$ .

The experiment was performed using as the pumping source a CW fiber-coupled diode laser (Apollo Instruments Inc.,  $\lambda = 940\text{ nm}$ ,  $100\text{ }\mu\text{m}$  core,  $\text{NA} = 0.2$ ,  $M^2 = 50$ ). The Yb:KGW crystal with 3 at.% doping was Ng-axis cut, had dimensions of  $3 \times 3 \times 4\text{ mm}^3$  and coatings with  $R < 10\%$  for 943 nm and  $R < 0.2\%$  for 1020–1120 nm. It was mounted in a copper housing using indium foil and water cooled to  $8\text{ }^\circ\text{C}$ . The 29 mm long hemispheric cavity was composed of a concave input mirror with radius-of-curvature of 50 mm and reflectivity of  $R(0^\circ, 1020\text{--}1200\text{ nm}) > 99.99\%$ , and a plane output coupler with  $R(1030\text{--}1080\text{ nm}) > 99.95\%$  and transmission of 0.15% at the first Stokes wavelength of 1096 nm. To focalize the pump beam into the crystal, a 15 mm focal length lens was used to collimate the beam exiting the fiber and another doublet lens of  $f = 30\text{ mm}$  was used to generate a focus of  $170\text{ }\mu\text{m}$  inside the KGW. Optical system losses from the diode output to the crystal pump facet were 10%. The cavity representation can be seen in Fig. 2.

Fundamental laser emission was observed at different wavelengths, initiating at 1047 nm and increasing in wavelength depending on the cavity alignment [20]. When the cavity was well aligned, we observed an emission centered at 1077 nm with a spectral width (FWHM) of 6 nm as shown in Fig. 1b. This happens because, in a quasi-three-level medium, the wavelength of the laser is determined by the losses in the resonator and the balance between emission and reabsorption. At a fixed pump intensity and crystal length, more reabsorption is present at shorter emission wavelengths. Therefore, the cavity with smaller losses usually leads to lasing at longer wavelengths, because the higher stimulated decay rate causes faster repopulation of the lower laser level. As seen in the inset to the right of Fig. 1a, at 1090 nm there is still some

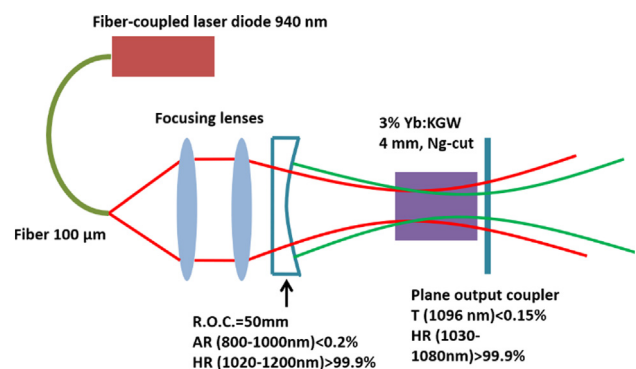


**Fig. 2.** Configuration of the laser setup. The red and green traces show the pump and laser beam, respectively, with their approximate beam waist position inside the crystal. (For interpretation of the references to colour in this figure legend, the reader is referred to the web version of this article.)

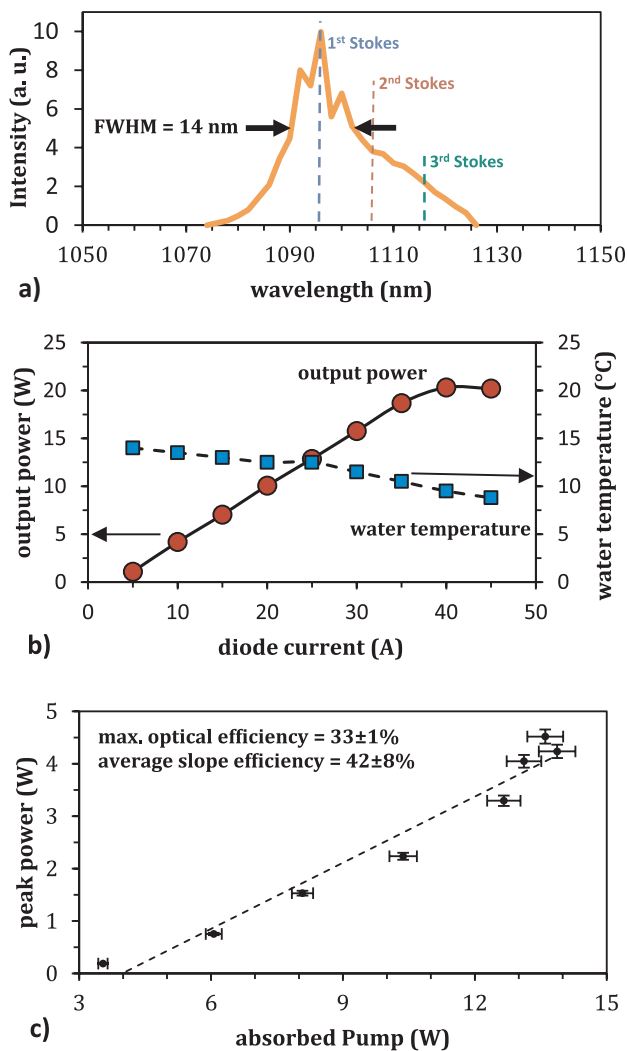


**Fig. 3.** (a) Emission spectrum of the Raman laser measured with a monochromator with 2 nm of resolution. The Stokes line was centered at 1096 nm and corresponds to the  $89\text{ cm}^{-1}$  conversion of the fundamental emission at 1086 nm. Also shown (vertical dashed lines) are the spectral positions of the second and third order Stokes shifts. (b) Output power (circles) of the diode and water temperature (squares) at the diode as a function of current. (c) Output power of the Raman laser emitting at 1096 nm. The dashed line is a linear data fit.

measurable gain left while absorption has dropped close to zero.

### 3. Results and discussions

When Stokes lasing was obtained, the fundamental emission (seen in Fig. 1b), was no longer observed at the output of the laser without changing the output coupler. This behavior of almost completely switching off the fundamental output in an abrupt manner, and also the characteristic, very broad fundamental spectra, have been observed before [13]. The Raman emission spectra, obtained by a diffraction grating monochromator with a resolution of 2 nm, can be observed in Fig. 3a. The Stokes emission is centered at 1096 nm. From the Raman shift of  $89\text{ cm}^{-1}$ , we calculate a fundamental center wavelength of 1086 nm. The very broad emission of 14 nm FWHM and 36 nm at  $1/e^2$  of the peak value extends to 1125 nm, and suggests cascaded Raman lasing with at least one overlapping higher order Stokes mode at 1106 nm, as shown in Fig. 3a. We note that even when using high reflectivity mirrors, which extend to the 1200 nm wavelength range and that, in principle, would allow for the  $768\text{ cm}^{-1}$  and  $901\text{ cm}^{-1}$  Raman

shifts of the Ng-axis cut crystal, no oscillation at the respective Stokes wavelengths was observed. This was expected, considering the much higher SRS cross-section of the  $89\text{ cm}^{-1}$  Stokes conversion for fundamental and Raman fields parallel to the  $N_m$  crystal axis and propagation along the Ng-axis [7].

The pump laser had issues in terms of the output spectra and also showed fast degradation of the output power, starting with 33 W at the beginning of the experiment and ending with 21 W at the time the final results were taken. Water temperature at the diode was adjusted for each output power in order to temperature tune the diode emission to the crystal's absorption peak at 934 nm (Fig. 3b). The pump spectra showed two peaks at powers up to 19 W (40 A) and split up into three peaks, as shown in Fig. 1a (left inset), at the maximum diode current of 45 A (see Fig. 3b) when the largest spectral overlap with the crystal absorption spectra was achieved, resulting in 74% of absorbed incident pump light. The diode's output power curve, shown in Fig. 3b, displays a roll over at the maximum pump current, probably due to heating of the fiber coupler, emitting 20.6 W at 40 A and 20.2 W at 45 A. Therefore, the highest laser output power of 4.5 W at 45 A is achieved at a slightly smaller absorbed pump power of 13.6 W, as can be seen in Fig. 3c, and is due to the better spectral overlap at 45 A.

The output of the pump laser was mechanically chopped to produce 1 ms pulses at 100 Hz repetition rate. Given the upper state lifetime of Yb:KGW of 0.6 ms, this can be regarded as CW operation from the population dynamics point of view. In terms of crystal fracture limit, it is noteworthy that crystals with much smaller fracture limit and much higher fractional heating have been continuously operated using approximately the same maximum absorbed pump power in a similar end-pumped Raman laser set-up. For example, a Nd:YLF/KGW laser (160 MPa fracture limit and 35% fractional heating) has been operated continuously with 12.3 W of absorbed pump power, demonstrating no fracture and no decrease in laser efficiency when compared to quasi-CW operation [21].

The efficiency curve for the Raman emission at 1096 nm is shown in Fig. 3c. The linear fit of Fig. 3c, shown by the dashed line, does not represent a best fit, but is included in order to determine an average slope efficiency. A slope efficiency of  $42 \pm 8\%$  and a best diode-to-Raman conversion efficiency of  $33 \pm 1\%$  at 13.6 W of absorbed pump power were obtained, with a maximum output power of 4.5 W. Because of the quasi-CW operation of our laser, the output power was very stable and the measurement error was the detector error (3%; Thorlabs, model 307C) [22]. The slope efficiency reported in Ref. [13] is in terms of incident pump power, which is the same as the absorbed pump power, given the pump wavelength and crystal parameters used in their set-up. We may, therefore, compare the efficiency of [13] with our obtained efficiency that is twice as high. We credit this result mainly to the lower doping concentration and smaller crystal length of the Yb:KGW, reducing reabsorption losses.

### 4. Conclusions

The relatively wide fundamental and Raman output spectra demonstrate multi-mode operation behavior, which is typical of these lasers and may severely hamper the maximum achievable output power [16]. An 'unclamped' fundamental field that continues to increase for pump powers above Raman threshold decreases laser efficiency at the fundamental and Stokes wavelengths [19]. It is expected that efficiency can be improved if a suitable etalon is introduced into the cavity to limit spectral bandwidth at the fundamental [23]. The separation of the pump from the Stokes wavelength could be accomplished by introducing into the cavity an additional mirror, highly reflective for the Stokes wavelength and highly transmissive for the pump and fundamental wavelengths, inserted before the crystal and after the pump mirror and the etalon. Finally, such a high gain SRL with fundamental line width limiting could be of interest for multi-wavelength laser sources by obtaining a frequency comb with several higher-order Stokes frequencies

that are closely spaced by  $89\text{ cm}^{-1}$ .

## Funding

We thank the São Paulo State Foundation FAPESP for grant 2017/10765-5 and the National Council for Scientific and Technological Development CNPq for the scholarship of MSc. Merilyn Ferreira, grant 1420502015-6.

## Acknowledgment

We would like to thank Dr. Helen Pask for helpful discussions.

## References

- [1] A.A. Demidovich, A.S. Grabtchikov, V.A. Lisinetskii, V.N. Burakevich, V.A. Orlovich, W. Kiefer, Continuous-wave Raman generation in a diode-pumped  $\text{Nd}^{3+}:\text{KGd}(\text{WO}_4)_2$  laser, *Opt. Lett.* 30 (2005) 1701–1703, <https://doi.org/10.1364/OL.30.001701>.
- [2] A.S. Grabtchikov, A.N. Kuzmin, V.A. Lisinetskii, G.I. Ryabtsev, V.A. Orlovich, A.A. Demidovich, Stimulated Raman scattering in  $\text{Nd}:\text{KGW}$  laser with diode pumping, *J. Alloys Compd.* 300–301 (2000) 300–302, [https://doi.org/10.1016/S0925-8388\(99\)00728-8](https://doi.org/10.1016/S0925-8388(99)00728-8).
- [3] Y.F. Chen, High-power diode-pumped actively Q-switched  $\text{Nd}:\text{YVO}_4$  self-Raman laser: influence of dopant concentration, *Opt. Lett.* 29 (2004) 1915–1917, <https://doi.org/10.1364/OL.29.001915>.
- [4] P. Dekker, H.M. Pask, D.J. Spence, J.A. Piper, Continuous-wave, intracavity doubled, self-Raman laser operation in  $\text{Nd}:\text{GdVO}_4$  at 586.5 nm, *Opt. Exp.* 15 (2007) 7038–7046, <https://doi.org/10.1364/OE.15.007038>.
- [5] M. Pollnau, P.J. Hardman, M.a. Kern, W.a. Clarkson, D.C. Hanna, Upconversion-induced heat generation and thermal lensing in  $\text{Nd}:\text{YLF}$  and  $\text{Nd}:\text{YAG}$ , *Phys. Rev. B* 58 (1998) 16076–16092, <https://doi.org/10.1103/PhysRevB.58.16076>.
- [6] I.V. Mochalov, Laser and nonlinear properties of the potassium gadolinium tungstate laser crystal  $\text{KGd}(\text{WO}_4)_2:\text{Nd}^{3+}-(\text{KGW}:\text{Nd})$ , *Opt. Eng.* 36 (1997) 1660–1670.
- [7] S. Sarang, R.J. Williams, O. Lux, O. Kitzler, A. McKay, H. Jasbeer, R.P. Mildren, High-gain 87 cm-1 Raman line of KYW and its impact on continuous-wave Raman laser operation, *Opt. Exp.* 24 (2016) 21463–21473, <https://doi.org/10.1364/OE.24.021463>.
- [8] J.J. Neto, C. Artlett, A. Lee, J. Lin, D. Spence, J. Piper, N.U. Wetter, H. Pask, Investigation of blue emission from Raman-active crystals: its origin and impact on laser performance, *Opt. Mater. Exp.* 4 (2014) 889, <https://doi.org/10.1364/ome.4.000889>.
- [9] N.V. Kuleshov, A.A. Lagatsky, V.G. Shcherbitsky, V.P. Mikhailov, E. Heumann, T. Jensen, A. Diening, G. Huber, CW laser performance of Yb and Er, Yb doped tungstates, *Appl. Phys. B* 64 (1997) 409–413, <https://doi.org/10.1007/s003400050191>.
- [10] A. Lagatsky, N. Kuleshov, V. Mikhailov, Diode-pumped CW lasing of Yb:KYW and Yb:KGW, *Opt. Commun.* 165 (1999) 71–75, [https://doi.org/10.1016/S0030-4018\(99\)00232-1](https://doi.org/10.1016/S0030-4018(99)00232-1).
- [11] V.E. Kisel, A.E. Troshin, N.A. Tolstik, V.G. Shcherbitsky, N.V. Kuleshov, V.N. Matrosova, T.A. Matrosova, M.I. Kupchenko, Q-switched Yb $^{3+}:\text{YVO}_4$  laser with Raman self-conversion, *Appl. Phys. B* 80 (2005) 471–473, <https://doi.org/10.1007/s00340-005-1749-x>.
- [12] J. Liu, U. Griebner, V. Petrov, H. Zhang, J. Zhang, J. Wang, Efficient continuous-wave and Q-switched operation of a diode-pumped Yb:KLu(WO $_4$ ) $_2$  laser with self-Raman conversion, *Opt. Lett.* 30 (2005) 2427–2429, <https://doi.org/10.1364/OL.30.002427>.
- [13] M.T. Chang, W.Z. Zhuang, K.W. Su, Y.T. Yu, Y.F. Chen, Efficient continuous-wave self-Raman Yb:KGW laser with a shift of  $89\text{ cm}^{-1}$ , *Opt. Exp.* 21 (2013) 24590, <https://doi.org/10.1364/OE.21.024590>.
- [14] D. Geskus, J. Jakutis Neto, S.-M. Reijn, H.M. Pask, N.U. Wetter, Quasi-continuous wave Raman lasers at 990 and 976 nm based on a three-level Nd:YLF laser, *Opt. Lett.* 39 (2014) 2982–2985, <https://doi.org/10.1364/OL.39.002982>.
- [15] N.U. Wetter, A.M. Deana, I.M. Ranieri, L. Gomes, S.L. Baldochi, Influence of excited-state-energy upconversion on pulse shape in quasi-continuous-wave diode-pumped Er:LiYF $_4$  lasers, *IEEE J. Quant. Electron.* 46 (2010) 99–104, <https://doi.org/10.1109/JQE.2009.2028305>.
- [16] D. Geskus, J. Jakutis-Neto, D.J. Spence, H.M. Pask, N.U. Wetter, Extreme linewidth broadening in a Nd:YLiF $_4$ -KGW intracavity Raman laser, 2015 Eur. Conf. Lasers Electro-Optics - Eur. Quantum Electron. Conf. Optical Society of America, Munich, 2015 p. CA\_P\_9.
- [17] N.U. Wetter, A. Berezcki, J.P.F. Paes, Quasi-three level Nd:YLF fundamental and Raman laser operating under 872-nm and 880-nm direct diode pumping, *Proc. SPIE - Int. Soc. Opt. Eng.* 2018, <https://doi.org/10.1117/12.2290444>.
- [18] C.C. Kores, J. Jakutis-Neto, D. Geskus, H.M. Pask, N.U. Wetter, Diode-side-pumped continuous wave Nd $^{3+}:\text{YVO}_4$  self-Raman laser at 1176 nm, *Opt. Lett.* 40 (2015) 3524, <https://doi.org/10.1364/OL.40.003524>.
- [19] D.J. Spence, Spatial and spectral effects in continuous-wave intracavity Raman lasers, *IEEE J. Sel. Top. Quant. Electron.* 21 (2015) 134–141, <https://doi.org/10.1109/JSTQE.2014.2344042>.
- [20] P. Dekker, J.M. Dawes, P.A. Burns, H.M. Pask, J.A. Piper, T. Omatsu, Power scaling of cw diode-pumped Yb:KGW self-Raman laser, 2003 Conf. Lasers Electro-Optics Eur. (CLEO/Europe 2003) (IEEE Cat. No.03TH8666), 2003, p. 50, <https://doi.org/10.1109/CLEO.2003.1312112>.
- [21] J. Jakutis-Neto, J. Lin, N.U. Wetter, H. Pask, Continuous-wave watt-level Nd:YLF/ KGW Raman laser operating at near-IR, yellow and lime-green wavelengths, *Opt. Exp.* 20 (2012), <https://doi.org/10.1364/OE.20.009841>.
- [22] N.U. Wetter, E.C. Sousa, F.D.A. Camargo, I.M. Ranieri, S.L. Baldochi, Efficient and compact diodeside-pumped Nd:YLF laser operating at 1053 nm with high beam quality, *J. Opt. A* 10 (2008) 104013, <https://doi.org/10.1088/1464-4258/10/10/104013>.
- [23] Q. Sheng, A. Lee, D. Spence, H. Pask, Wavelength tuning and power enhancement of an intracavity Nd:GdVO $_4$ -BaWO $_4$  Raman laser using an etalon, *Opt. Exp.* 26 (2018) 32145–32155, <https://doi.org/10.1364/OE.26.032145>.